

Performance evaluation of PSD for silicon ECAL

Hiroaki Yamashiro, Kiyotomo Kawagoe, Taikan Suehara, Tamaki Yoshioka,
Yuji Sudo, Hiroki Sumida

Kyushu University

March 24, 2017

Abstract

We are developing position sensitive silicon detectors (PSD) which have an electrode at each of four corners so that the incident position of a charged particle can be obtained using signals from the electrodes. It is expected that the position resolution the electromagnetic calorimeter (ECAL) of the ILC detector will be improved by introducing PSD into the detection layers. In this study, we irradiated collimated laser beams to the surface of the PSD, varying the incident position. We found that the incident position can be well reconstructed from the signals if high resistance is implemented in the p+ layer. We also tried to observe the signal of particles by placing a radiative source on the PSD sensor.

1 Introduction

International Linear Collider (ILC) is a next generation linear collider whose construction plan is progressing to search for new physics. International Large Detector (ILD) [1] is one of the detector concept for ILC. Particle Flow Algorithm [2] is the key analysis method used in ILC. In PFA, particles in the jets are separated and the optimal detector is used to measure individual particles. The momenta of charged particles are measured by the tracker, energies of photons are measured by the electromagnetic calorimeter, and energies of neutral hadrons are measured by the hadron calorimeter. To improve the performance of PFA, it is necessary to distinguish the particles in the jet.

Figure 1 shows ECAL of ILD. The electromagnetic calorimeter (ECAL) of ILD, which is a sampling calorimeter composed of tungsten absorber layers and segmented sensor layers. In the ECAL, it is necessary to separate the particles in an electromagnetic shower one by one in order to satisfy the PFA requirement, so we should improve the position resolution of the detection layer of ECAL as much as possible. For this purpose, highly segmented silicon pad sensor are employed as the reference design of ILD ECAL. We are investigating position sensitive silicon detector (PSD) for an alternative design to further improve the position resolution of photons.

Talk presented at the International Workshop on Future Linear Colliders (LCWS16), Morioka, Iwate, 5-9 December 2016.

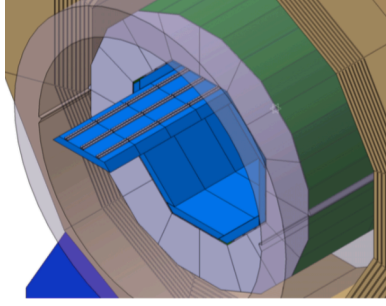


Figure 1: ILD ECAL (blue area) [1].

2 About PSD

Figure 2 shows the schematic of the cross section of silicon sensors [3, 4]. Electrons and holes are generated along the path of a charged particle. In conventional silicon pads, the charge goes through p^+ pad to electrodes. In PSDs, the charge reaches a p^+ surface at first, then running through the resistive p^+ surface to the electrodes. This divides the charges by resistive division, so we can calculate the incident position from the function of the charge recorded at each electrode. This mechanism gives higher position resolution without further dividing electrodes.

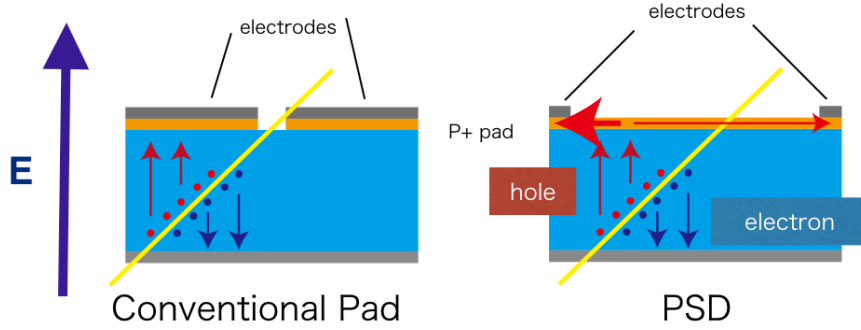


Figure 2: Sectional view. (Right: Conventional sensor, Left:PSD sensor)

PSD sensors are expected to enhance the function of ILD ECAL by improving position resolution of photons. PSDs can be used at the innermost layers of ECAL where hit density is much smaller than the shower maximum region. We can employ larger cell sizes for those layers to avoid increasing number of readout channels, considering PSD needs four electrodes on one cell. We expect less than 1 mm position resolution with PSD in 1 cm^2 cells, which is significantly less than the resolution with conventional pads of $5 \times 5 \text{ mm}^2$ cells.

There are advantages of having better position resolution in ECAL. First, the reconstruction of π^0 from two photons can be improved. The improved position resolution can be used for the kinematic fit of π^0 reconstruction, which leads to improve the jet energy resolution and reconstruction of heavy quarks (b/c tagging).

PSDs can also be used for strip tracking detectors in order to reduce ghost hits by obtaining hit positions roughly along the strips. Effects on physics performance should be confirmed with Monte-Carlo simulation study. The size of PSD sensors is 7.0 times 7.0 mm. Thickness is $320 \mu\text{m}$. No guard rings are implemented on the edges of the sensors.

Figure 3 shows a PSD sensor made by Hamamatsu Photonics. This sensor has electrodes at the four corners.

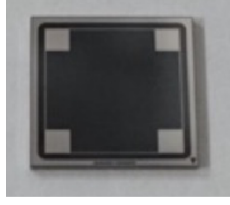
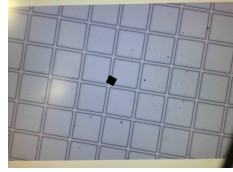


Figure 3: The PSD sensor.

We have two types of PSD sensors. The difference between the two types can be seen by a microscope. Figure 4a and 4b are the magnified views of the black areas of Fig.3 for the two types of sensors. This mesh increases the resistivity of the p^+ layer. With the larger resistivity, it is expected to reduce the noise and the position distortion. Flat surface of the p^+ layer is seen on Figure 4b, in contrast to Figure 4a, which shows meshed p^+ surface.



(a) meshed p^+ layer



(b) non-meshed p^+ layer

Figure 4: magnified picture of PSD

Figure 5a and 5b are the result of capacitance measurement characteristics of PSD with mesh and PSD without mesh, respectively. They are fully depleted at about 60 V and 50 V, respectively.

Figure 6 is a printed circuit board (PCB) and a holder for four sensors. This is called “sensor box” below. In this picture two of the four sensor places are filled with a meshed and a non-meshed sensor. The box was fixed in a two axis automatic stage in a dark chamber as shown in Figure 7 and reverse bias of 100 V was applied to the sensors.

3 Evaluation of Detecting Position using Laser

Laser photons were injected to the PSD sensors to test the position reconstruction. The specifications of the laser are shown in Table 1.

The PCB on the sensors has cut on the main part of PSD sensors to pass the laser photons through it. Since the photon energy is slightly higher than the band gap energy of silicon, one optical photon creates one electron-hole pair in the silicon, and imitate signal at the well defined position. The movable stage below the sensor box was used to control the injection position.

Figure 8 shows a schematic diagram of data acquisition system (DAQ). Signal from each electrode was amplified by a preamplifier and a shaper, and delivered to a peak-hold ADC module on a CAMAC system. The gate signal of the ADC was applied from the laser injection

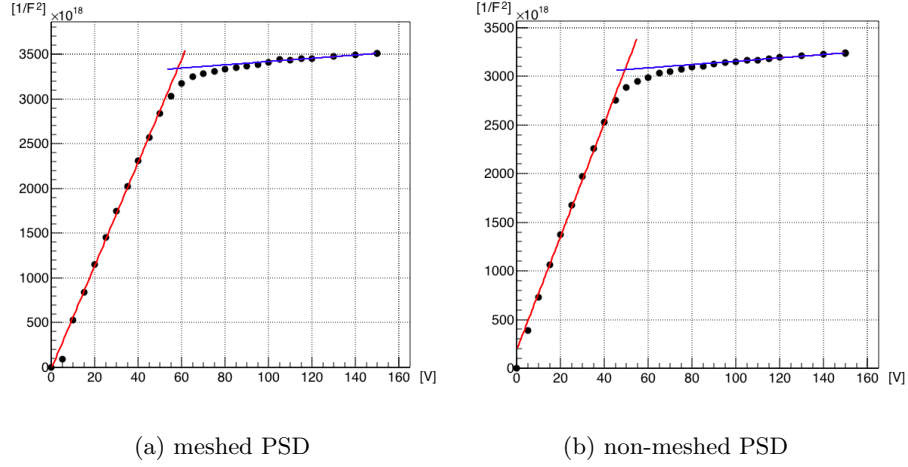


Figure 5: C-V characteristics

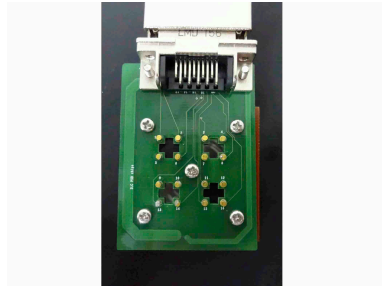


Figure 6: Sensor Box

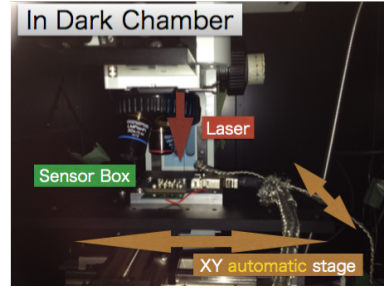


Figure 7: Sensor Box fixed on XY stage

trigger. We accumulate 8000 pulses at one point, and average the ADC counts over the pulses. To calculate the position from signals, we use the following formulae [4],

$$\begin{aligned} X_{\text{rec}} &= \frac{(\text{ch5} + \text{ch6}) - (\text{ch7} + \text{ch8})}{\text{ch5} + \text{ch6} + \text{ch7} + \text{ch8}} \\ Y_{\text{rec}} &= \frac{(\text{ch6} + \text{ch8}) - (\text{ch5} + \text{ch7})}{\text{ch5} + \text{ch6} + \text{ch7} + \text{ch8}} \end{aligned} \quad (1)$$

where X_{rec} and Y_{rec} are reconstructed position along X and Y axis, and ch5-8 stand for ADC counts after the pedestal subtraction, as shown in Fig. 9.

3.1 Measurement result of meshed PSD

Figure 10a shows real injection positions, obtained from the positions of the two-axis stage. The red points are the point with sufficiently strong signals of 1000 or more ADC counts on all channels. A black cross mark indicates that the ADC output value of one or more channels is

Type	GryLaS IQ-1064-2
Wavelength	1064 nm
Laser intensity	20 μ J, reduced by NID fliters to 50 MIP equivalent.
Pulse duration	1.2 ns
Repetition rate	1000 Hz
Laser spot size	less than 20 μ m

Table 1: The specifications of the laser and optics

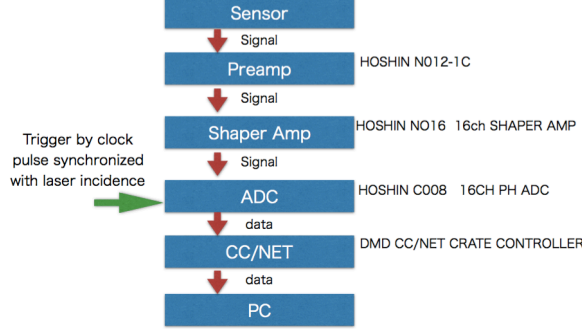


Figure 8: A schematic diagram of the DAQ

smaller than 1000 so that the signal is too weak to be reconstructed. This plot should reflect the shape of the open cut of the sensor box if the sensor is fully active.

Figure 10b shows reconstructed positions by Eq.1. In this figure, only points with sufficient signal strength are plotted. Distortion from the original grid, which is expected behavior of PSDs, is seen.

Figure 11a and 11b are the correlation between the actual incident position and the reconstructed position of the X and Y coordinates, respectively. A good correlation between the two positions with some non-uniformity is obtained.

3.2 Measurement result of non-meshed PSD

The same measurement was performed on the non-meshed PSD, shown in figure 12a. Shapes like open cut of sensor box are seen. However, strong signals cannot be obtained at two places surrounded by an ellipse, and the reason is under investigation.

Figure 10b shows reconstructed positions. Compared with the meshed PSD, the reconstructed positions are concentrated in the almost same value.

This shows that the non-meshed PSDs are not functional to obtain the incident positions.

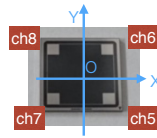


Figure 9: Assignment of channels on the PSD electrode.

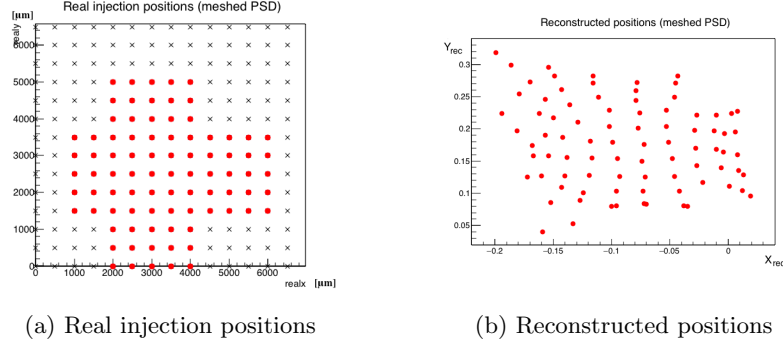


Figure 10: Measurement result of meshed PSD

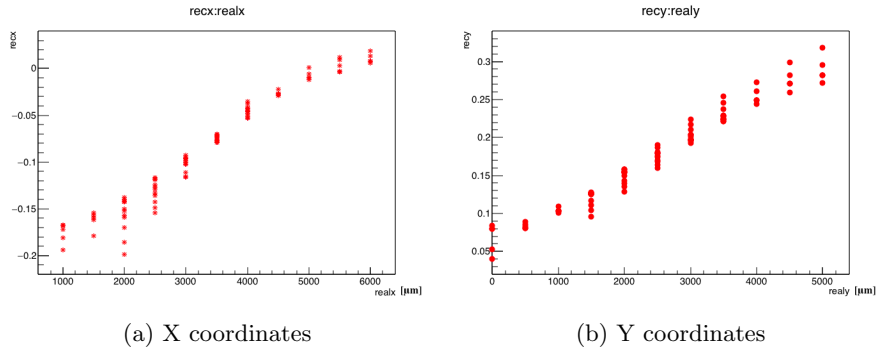


Figure 11: The correlation result of meshed PSD

The high resistivity of p^+ layer should be essential for this type of PSDs.

4 A noise measurement using β source

As shown in Figure 13, a rubber sheet of 1 mm thickness was put on the sensor box, and ^{90}Sr was put on the rubber sheet. That was done with a conventional pixel type silicon sensor and PSD with mesh, respectively, and we tried to capture the signal with the radiation source.

Figure 14 shows a schematic diagram of DAQ to capture the signal with the radiation source. ADC was self-triggered. Signals are inverted in the shaper amplifier to make the trigger. For the PSD sensor, measurement was carried out for 2 hours in a state with and without a radiation source. During this time, the sum of the signals from four electrodes after passing shaper amplifier from the four electrodes exceeded 400 mV was treated as an event. In the pixel type silicon sensor, 4 pixels out of 9 pixels were used in a state with a radiation source. When the signal of 1 pixel exceeded 100 mV, it was treated as an event. At this time, the output values of the other three pixels are recorded as a pedestal.

Figure 15 is the distribution of the ADC output in one pixel of a conventional pixel type silicon sensor. It seems that the signal from the beta source on the right side of the plot and the pedestal on the left seem to be separated well, but it seems to be seen separately by the trigger.

Figure 16 is the distribution of the sum of the ADC outputs from the four electrodes of PSD with and without radiation source. This shows that the signal comes more frequently with

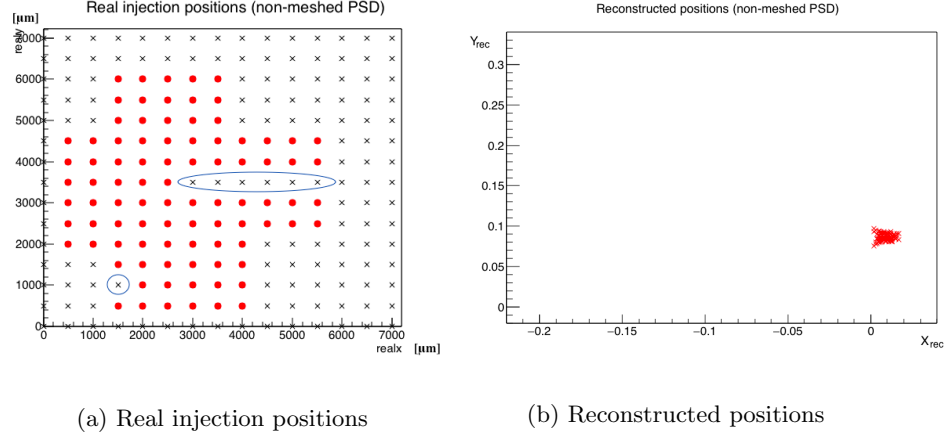


Figure 12: Measurement result of non-meshed PSD

radiation source than without, however the difference on the distribution is not clear, mainly due to a noise coherent to all channels. We plan to reduce this system noise in the future and try again to measure the radiation source.

5 Summary

PSD is a silicon device which can derive the incident position of a particle by resistive division of the charge to electrodes at the p^+ surface. It is expected PSDs at the innermost layers of ECAL to improve the position resolution of photons. Our first sample shows reasonable reconstruction of incident position of laser photons with some distortion. Meshed p^+ surface gives better result. Studies on the noise is ongoing.

The silicon pads measured in this study have no gain. Silicon sensors with avalanche gain are recently developed and is expected to obtain position resolution less than $100 \mu\text{m}$. We plan to reduce electronic noise for PSD measurement, create PSD sensors with avalanche gain, and confirm effects on physics performance with Monte-Carlo simulation study.

Acknowledgements

We appreciate that J-PARC muon g-2/EDM collaboration supported in production of the PSD sensors, and Hamamatsu Photonics suggested meshed PSD sensor.

References

- [1] T. Behnke, James E. Brau, Philip N. Burrows, M. Peskin, et al, The International Linear Collider Technical Design Report - Volume 4: Detectors. 2013, arXiv:1306.6329
- [2] M.A. Thomson, Particle Flow Calorimetry and the PandoraPFA Algorithm. Nucl. Instrum. and Meth A611 (2009) 25-40
- [3] <http://www.hamamatsu.com/resources/pdf/ssd/e02_handbook_si_photodiode.pdf> [Accessed 20 March 2017]

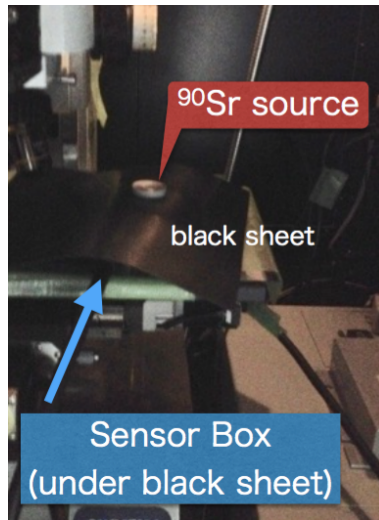


Figure 13: Radiation source put in the Sensor box

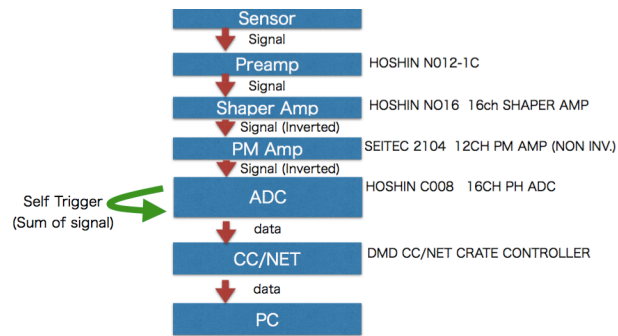


Figure 14: A schematic diagram of DAQ to capture the signal by the radiation source

- [4] A. Banu, Y. Li, M. McCleskey, M. Bullough, S. Walsh, C.A. Gagliardi, L. Trache, R.E. Tribble, C. Wilburn, Performance evaluation of position-sensitive silicon detectors with four-corner readout. Nucl. Instrum. and Meth A593(3), (2008) 399-406

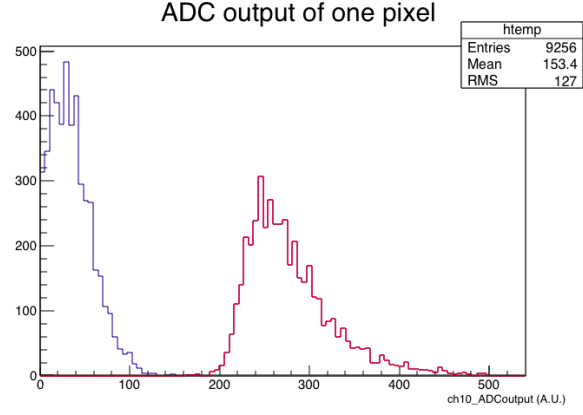


Figure 15: The distribution of the ADC output in one pixel of a conventional pixel type silicon sensor. (Red: Signal from radiation source Blue: Pedestal)

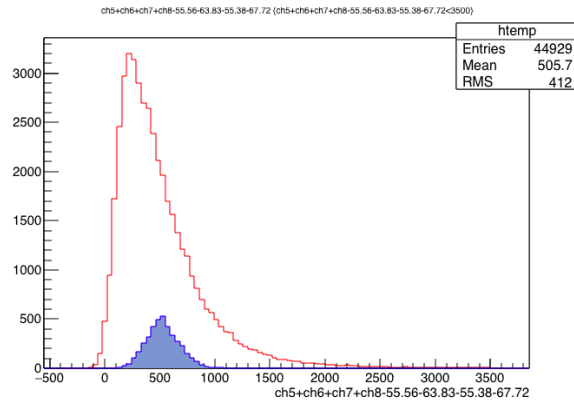


Figure 16: The distribution of the sum of the ADC outputs from the four electrodes of PSD (Red: with radiation source Blue: without radiation source)